Int J Adv Manuf Technol (2014) 74:163–185
DOI 10.1007/s00170-014-5975-4

ORIGINAL ARTICLE

A study on optimal design of process parameters in single point incremental forming of sheet metal by combining Box–Behnken design of experiments, response surface methods and genetic algorithms

R. Bahloul · H. Arfa · H. BelHadjSalah

Received: 10 October 2013 / Accepted: 18 May 2014 / Published online: 29 May 2014

Abstract Incremental forming is a sheet metal forming process characterized by high flexibility; for this reason, it is suggested for rapid prototyping and customized products. On the other hand, this process is slower than traditional ones and requires in-depth studies to know the influence and the optimization of certain process parameters. In this paper, a complete optimization procedure starting from modeling and leading to the search of robust optimal process parameters is proposed. A numerical model of single point incremental forming of aluminum truncated cone geometries is developed by means of Finite Element simulation code ABAQUS and validated experimentally. One of the problems to be solved in the metal forming processes of thin sheets is the taking into account of the effects of technological process parameters so that the part takes the desired mechanical and geometrical characteristics. The control parameters for the study included wall inclination angle (α), tool size (D), material thickness (Th_{ini}), and vertical step size (In). A total of 27 numerical tests were conducted based on a 4-factor, 3-level Box–Behnken Design of Experiments approach along with FEA. An analysis of variance (ANOVA) test was carried out to obtain the relative importance of each single factor in terms of their main effects on the response variable. The main and interaction effects of the process parameters on sheet thinning rate and the punch forces were studied in more detail and presented in graphical form that helps in selecting quickly the process parameters to achieve the desired results. The main objective of this work is to examine and minimize the sheet thinning rate and the punch loads generated in this forming process. A first optimization procedure is based on the use of graphical response surfaces methodology (RSM). Quadratic mathematical models of the process were formulated correlating for the important controllable process parameters with the considered responses. The adequacies of the models were checked using analysis of variance technique. These analytical formulations allow the identification of the influential parameters of an optimization problem and the reduction of the number of evaluations of the objective functions. Taking the models as objective functions further optimization has been carried out using a genetic algorithm (GA) developed in order to compute the optimum solutions defined by the minimum values of sheet thinning and the punch loads and their corresponding combinations of optimum process parameters. For validation of its accuracy and generalization, the genetic algorithm was tested by using two analytical test functions as benchmarks of which global and local minima are known. It was demonstrated that the developed method can solve high nonlinear problems successfully. Finally, it is observed that the numerical results showed the suitability of the proposed approaches, and some comparative studies of the optimum solutions obtained by these algorithms developed in this work are shown here.

Keywords Incremental forming process · Finite element modeling · Optimization · Design of experiments · Response surface methodology · Genetic algorithm

1 Introduction

Incremental sheet forming (ISF) is a flexible process which does not need dedicated forming tools. A sheet of metal is formed by a progression of localized plastic deformation using a simple hemispherical tool, controlled by a CNC milling

R. Bahloul (✉) · H. Arfa · H. BelHadjSalah
Laboratoire de Génie Mécanique (LGM), Ecole Nationale d'Ingénieurs de Monastir (ENIM), Université de Monastir, Avenue Ibn Eljazzar, 5019 Monastir, Tunisia
e-mail: bahloul_riadh@yahoo.fr

machine-tool. The tool is moved over the surface of the sheet along contours, which follow the shape of the final geometry as described by CAD-CAM software. Upon the completion of a contour, the tool is moved to greater depth and the stylus like tool traces the next contour. Step by step the concept takes a physical form as a sheet metal part [1] and consequently, the final shape is built progressively according to the tool motion, such that a highly localized plastic deformation is caused. The cumulative effect of these local deformations leads to the desired final geometry. Thus, varied and complex 3D shapes can be achieved by moving the tool along a correctly designed path, without the need to manufacture specialized tools. As reported in [2, 3] several ISF configurations have been designed and studied. So, depending on the number of contact points between sheet, tool and die, it is possible to distinguish between two-point incremental forming (TPIF) with partial or full die, and single point incremental forming (SPIF).

This work is dedicated to the detailed development and the optimization of SPIF process for thin metal sheets in order to control some process parameters and to improve the final product quality. SPIF process is interesting both industrially and scientifically. It represents a die-less sheet metal forming process in which a peripherally clamped sheet is locally deformed using a simple hemispherical ended tool that follows a predefined toolpath [4, 5], controlled and performed on a CNC machine. A sketch of SPIF is presented in Fig. 1. It makes it possible to illustrate this concept of vertical incrementing.

Most investigations of SPIF process have concerned applications and formability limits of the process [6–8]. The experimental investigations [9] lead to the conclusion that the formability of the process can be defined in terms of four major parameters: tool velocity and radius, sheet thickness and forming strategy. In Arfa et al. [10] and Duflou et al. [11], the formability is determined by considering the evolution of forming forces during the process. This approach is based on force measurements during the production of conical part. Typical curves are reported and influences of some process parameters are revealed. Ambrogio et al. [12] used this approach to evaluate a “spy variable” for defining a correction strategy to prevent failure during process. For scientists, ISF exhibits local effects and needs then new characterization methods. Ham and Jeswiet [13, 14], have built forming limit diagrams by using a Box–Behnken design of experiments and response surfaces method based on the two following criteria: maximum forming angle and effective strains.

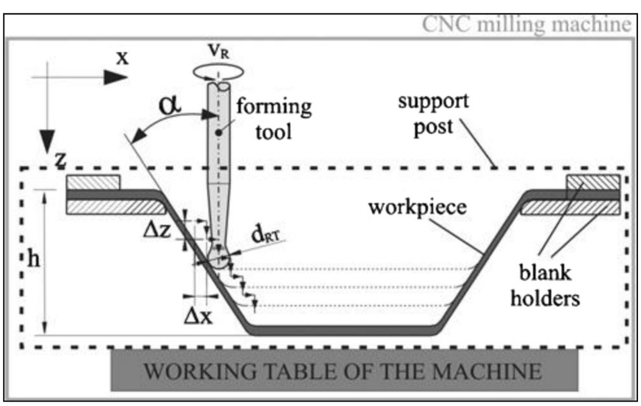

Fig. 1 Principle of single point incremental forming process (SPIF)

Through the last decades, it has been discovered that it is expensive and time consuming to design incremental sheet forming processes as well as conventional forming processes using trial and error. The application of numerical simulation based on the finite element method for single point incremental forming process helped engineers to efficiently improve the process development avoiding the cost and limitations of compiling a database of real world parts. Finite element analysis allows an inexpensive study of arbitrary combinations of input parameters including design parameters and process conditions to be investigated [15]. In this sense, Dejardin et al. [16] developed an experimental work and numerical modeling for improving knowledge of incremental sheet forming process for sheet metal parts. Their studies are related to the analysis of shape distortions and springback effects arising in single point incremental sheet forming in order to study the use of a FE model based on shell elements to perform simulation of the process. Thibaud et al. [17] have proposed a fully parametric toolbox for the simulation of single point incremental sheet forming process. Therefore, their work is dedicated to the development of SPIF for microparts (shape or detail) and for thin metal sheets (less than 1 mm). The complete methodology is proposed and numerical results are presented in terms of global geometry (shape and section profiles), thickness evolution and forming forces. Equivalent experimental tests are carried out to validate the numerical approach. Previous researches by Bouffioux et al. [18] demonstrated an experimental and numerical study of an AlMgSc sheet formed by an incremental process, since this material, which is well adapted to the aeronautic domain, is poorly known. A numerical model was developed and proved to be able to predict both the force evolution during the process and the final geometrical shape. The first objective is to reach a better knowledge of this alloy to provide the missing useful information to the aeronautic industry. The second objective is to study the applicability of the SPIF process on this material. The numerical inaccuracy of finite element models is one of the main problems often encountered by scientists. Furthermore, the simulations usually require a very high computation time because the tool path is long and can be complex. The combination of different strategies described by Bouffioux et al. [19, 20], Lequesne et al. [21] to improve the material and numerical models and applied on this study aims to be able to accurately simulate the process with a short computation time. Numerical simulations are very useful to develop manufacturing processes (feasibility, optimization). Therefore, numerical simulations based on the finite element method have been carried out for developing ISF process. Henrard et al. [22, 23] have performed studies to propose the best ways for numerical modeling to predict the process correctly. Malhotra et al. [24] have investigated the use of several material models and element formulations to simulate SPIF. From these studies, it has been shown that element formulations (solid element), integration algorithms (transient dynamic explicit algorithm), material models and contact algorithms are the most influent parameters.

The optimization of forming processes aimed at the production of net-shape components and high resistant products is nowadays one of the fundamental topics on which the interest of automotive research groups is focused. Some papers related to the optimization of forming strategies in ISF process have been published [25–27]. As a reliable methodology, design of experiments [13, 28] and response surface approximation [29] are retained in several cases for analysis and optimization of sheet metal forming. In 2008, an application to the optimization of sheet metal forming processes by adaptive response surface based on intelligent sampling method was given by Wang et al. [30]. The study of Azaouzi and Lebaal [31] proposes an optimization procedure tested for tool path optimization in single point incremental sheet forming using response surface method, in order to reduce the manufacturing time and homogenize thickness distribution of an asymmetric part. The optimal forming strategy was determined by finite element analyses (FEA) in combination with response surface method (RSM) and sequential quadratic programming (SQP) algorithm. In [26, 32], Attanasio et al. presented in their work the optimization of the tool path in two point sheet incremental forming with full die, in a particular asymmetric sheet incremental forming configuration. The aim of the study was the experimental evaluation and optimization of the tool path, which is able to reproduce an automotive component with the best dimensional accuracy, the best surface quality and the lowest sheet thinning. Sun et al. [33] developed a multiobjective robust optimization method to address the effects of parametric uncertainties on drawbead design in sheet metal forming, where the six sigma principle is adopted to measure the variations, a dual response surface method is used to construct surrogate model and a multiobjective particle swarm optimization is developed to generate robust Pareto solutions. An innovative monitoring and control approach, aimed to define and in process update the most relevant process parameters during an industrial SPIF operation, is proposed [34]. The experiments were designed according to a CCD face-centered plan; a suitable statistical analysis was carried out on the obtained results, permitting to highlight the influence of the experiment parameters on the punch force trend and, what is more, on the force gradient which occurs after the force peak. Furthermore a critical value of the mentioned gradient was determined for the investigated material, as function of the sheet thickness.

Some papers have tried to establish a new approach for numerical optimization problems in the field of manufacturing. They suggest using genetic algorithms (GA) [35] recently applied as an approach to sweep a region of interest and select the optimal (or near optimal) settings to a process [36]. Liu et al. [37] proposed a technique based on artificial neural network (ANN) and GA to solve the problem of springback of the typical U-shaped bending. The results show that more accurate prediction of springback can be acquired with the GA-ANN model. It can be taken as a reference for sheet metal forming. A study on the relation of springback and various process parameters was carried out based on the model of springback, providing theoretical guide for sheet metal forming and tools design. A Pareto-based multiobjective genetic algorithm was applied to optimize sheet metal forming process has been investigated by Wei et al. [38]. An optimal design is performed for powder die-pressing process based on the genetic algorithm approach [39]. It includes the shape optimization of powder component, the optimal design of punch movements, and the friction optimization of powder–tool interface. The goal of the optimization is to eliminate the work-piece defects that may arise during the powder compaction process. Ledoux et al. [40] have developed an optimization method and a numerical model for stamping tools under reliability constraints through finite element simulation codes and validated by experimental methods. The search for optimal tool configurations is performed by optimizing a desirability function and by means of a genetic algorithm based optimization code. Many works have been developed in order to optimize many forming processes of sheet metal. In fact, many researchers have applied an optimization strategy into manufacturing based on a combination of finite element method (FEM), ANN computation, and GA [37, 41–43].

In the present work, an optimization strategy for single point incremental sheet forming process based on finite element analysis, design of experiments, response surface methodology and genetic algorithm method is proposed. A model of SPIF part is developed through finite element simulation and validated by experimental methods. The major factors considered in SPIF are forming angle, punch diameter, initial sheet thickness and incremental step size. Accordingly, a Box–Behnken design of experiments (DOE) approach was used to study the sensitivity of predictions to four inputs of the forming process parameters. It also allows to develop the numerical plan, formalize the forming parameters critical in SPIF, and analyze data. The main effects and interaction plots of the four forming parameters on sheet thinning rate and the punch loads evolution are investigated by adopting the analysis of variance (ANOVA) technique. The steps of optimization procedure include the using of a global approach based on the response surface method to establish the mathematical models that represent the relationship between design factors and the objective functions, and the genetic algorithm to find the optimum solutions from the response surface generated. The ability of each technique to find the optimal solution is evaluated, and good results are obtained from these optimization techniques. Some conclusions are drawn from the numerical results.

2 Modeling and numerical analysis of the SPIF process

In this study, we consider the SPIF operations. This process is based on layered manufacturing principles, where the model is divided into horizontal slices. The numerically controlled (NC) tool path is prepared by using contours of these slices. It is a progressive sheet metal forming operation characterized by large displacements and strains, and located deformations. The punch is a simple-shaped tool with a diameter far smaller than the dimension of the part being made. Proceeding in an incremental way, the tool is moved along contours which follow the shape of the final geometry as described by CAD and CAM of CATIA software. It makes it possible to impose a local deformation on the sheet in a consecutive manner. In this investigation, elasto-plastic analysis of SPIF process by FEM was performed using a finite element code ABAQUS© software capable of handling large deformation. Finite element models are established to simulate aluminum-truncated cones. The output of the simulation is given in terms of the reaction forces, the final geometry and the thickness distribution of the product.

2.1 Incremental sheet forming conditions and material behavior

The sheet metal used in the numerical simulation is Al 3003-O [11]. It is considered as isotropic and the flow has been accounted by means of a Swift-type hardening law expressed as [44]:

$$\bar{\sigma} = \mathrm{k}(\varepsilon_0 + \bar{\varepsilon})^{\mathrm{n}} \tag{1}$$

where k is the strain hardening coefficient, n the power law coefficient and $\bar{\varepsilon}$ is the effective accumulated plastic strain. This choice has been validated through a tensile test that has been used to determine the material coefficients. The parameters are as follows: k=184 MPa, n=0.224 and ε_0=0.00196.

The elastic part of the constitutive behavior of the sheet is assumed to be linear and isotropic, with Young's modulus (E) and Poisson's ratio (ν) were taken to be 70.0 GPa and 0.33, respectively. The plasticity criterion of Hill was considered, and therefore the anisotropy phenomenon of material was introduced in the numerical models of the SPIF process. The planar anisotropies are characterized by experimental tests according to three particular directions. They are fitted according to measured Lankford coefficients: r_0=0.51, r_{45}=0.75, and r_{90}=0.48.

Modeling the interaction between the tool and the sheet is one of the most important considerations necessary to simulate the incremental forming process correctly. Concerning the processing conditions, tools are considered as an analytical rigid body and the corresponding boundary conditions are related to the defined path, while the sheet material is considered as elastic-plastic object. The contact at the interface between sheet and tools follows Coulomb's friction law:

$$\tau_{\mathrm{f}} = \mu \sigma_{\mathrm{n}} \tag{2}$$

where τ_f is friction shear stress, σ_n is normal stress at interface and μ is the friction coefficient. Friction conditions between the forming tool and the sheet metal part have been accounted by considering sliding friction with a friction coefficient equal to 0.09.

2.2 Finite element simulation of SPIF

As incremental forming is a progressive sheet metal forming process characterized by large displacements and large localized strains, therefore static simulations were conducted in this work by using the implicit FE package Abaqus/Standard like calculation algorithm. An axisymmetric part representative of right truncated cone at 40 mm depth with circular base having the initial diameter of D=180 mm obtained from a square blank sheet (200×200 mm) was studied considering the SPIF process. Figure 2 shows a generation of discontinuous tool path showing the forming of a cone. Each tool path is made up of a series of contours generated transverse to the long axis of the cone. The forming tool follows the predetermined tool path and gradually forms the sheet metal in a series of incremental steps until the final depth is reached. The tool motion is usually described in terms of Cartesian coordinates. The steps of single point incremental sheet metal forming are usually defined as Δx, Δy representing increments in horizontal sheet plane labeled as the X-axis and Y-axis and a finite forming depth h in vertical Z-axis respectively, being the direction in which deformation occurs.

The part is formed according to a discontinuous trajectory as it shown in Fig. 2. The tool starts from the outside of the shape toward the inner part and incrementally goes down in the Z-direction with increasing depth describing a sort of spiral until the desired diameter at the maximum depth is reached. In this way, the tangential movement of the tool completely forms the product profile. The tool path is prescribed by NC data that is generated from a CAD model of the component to be formed. The forming strategy consists of a single forming stage where the tool traces along a sequence of contour lines with a vertical increment step size in between. The part is

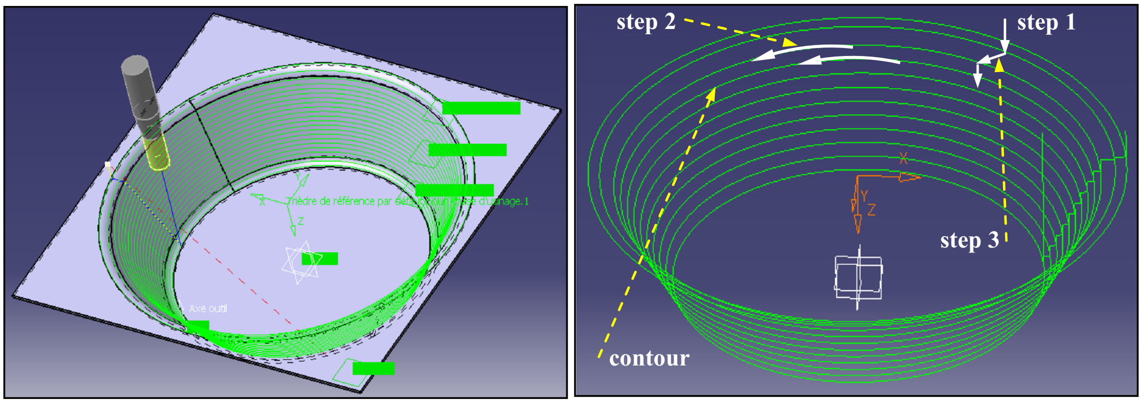

Fig. 2 Schematic description of the tooling path generated by CATIA and integrated into ABAQUS

formed progressively and locally around the tool thanks to its CNC-controlled movement. Using this forming strategy it is obvious that there are a relatively large number of adjustable process parameters that can influence the forming process for a given geometry such as the forming angle, the radius of the forming tool, the initial thickness of the sheet metal or the size of the step down.

As sheet metal forming involves large material rotation as well as strain, suitable algorithm should be employed in the FEA. Due to the 3D tool path movement, a fully three-dimensional, elasto-plastic FE model is set up for the simulation to investigate the SPIF process. Figure 3 reports the developed numerical model for the process in the initial, intermediate and final configurations of the part during the single point incremental operation. It shows both the undeformed and deformed shapes modeled in this context.

As a consequence, quadrilateral shell elements with 4 nodes and 6 degrees of freedom per node (S4R) and five Gaussian reduced integration points through the thickness direction were used. These elements are the so-called 3D reduced shell elements and are well suited to properly considered thickness variations through the deformation process. Consequently, they are widely used in the forming problems of large deformation and large rotation. The general shape of the aluminum alloy sheet Al 3003-O has been considered square for different thicknesses with a size of 200 mm× 200 mm. The finite element meshing subdivision of the initial blank is depicted in Fig. 4. The aluminum alloy sheet was modeled as an elasto-plastic material with isotropic hardening using material data previously mentioned. In the FE model, the blank was initially meshed with 25,600 rectangular shell finite element (dimensions, 1.25 mm×1.25 mm) considering reduced integration and 25,901 nodes.

The parameters of the finite element model (meshing, element type and contact algorithm) are selected after several numerical simulations to evaluate their influence on the computational time and to achieve good results. Particular attention has to be paid to the mesh conditions. In this particular simulation, the selection of the mesh is of great importance because it must be suitable to describe the precision the results. Therefore, a convergence study through mesh size reduction has been carried out for the finite element model. All simulations were performed on Windows XP PC Core 2 Quad with 2.5 GHz processor and a read/write memory performance of 2,096 Mb. The CPU time required to simulate the single point incremental forming process of truncated cone mentioned previously takes, on average, 5 days.

3 Design of numerical experiments

In order to effectively determine the correlations between the process parameters and the responses as well as in order to determine the optimal design variables in SPIF, a campaign of

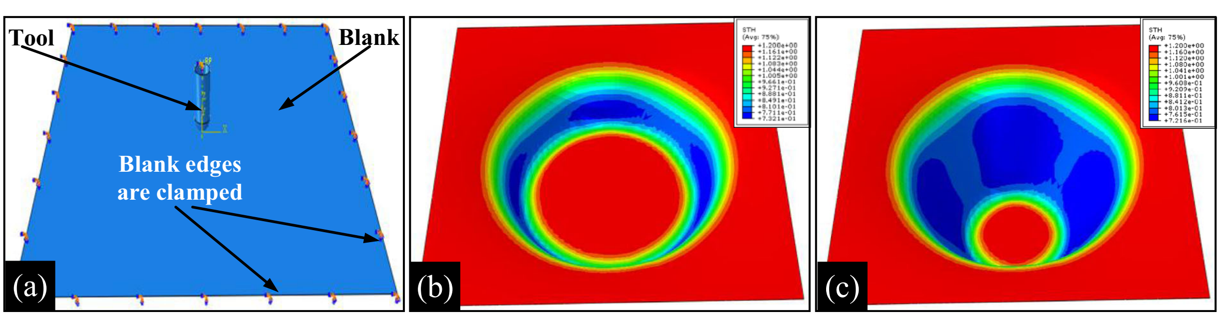

Fig. 3 Schematic of the setup in FEA simulations. **a** Initial, **b** intermediate, and **c** final configurations of the blank shape during the SPIF operation

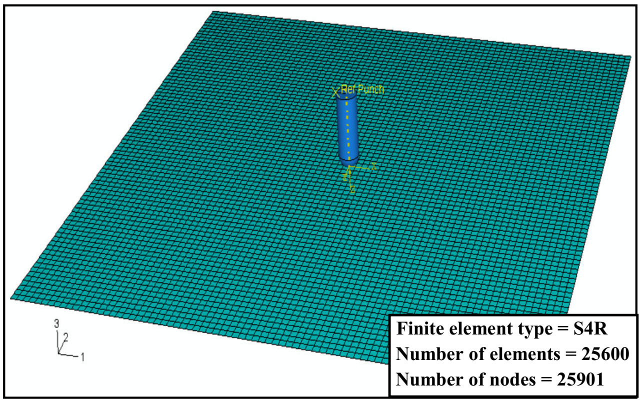

Fig. 4 Initial FE meshing configuration and tool position for the truncated cone simulation in ABAQUS formed by SPIF

numerical simulations using finite element analysis was carried out based on a proper DOE. A Box–Behnken experimental design [45] is executed using four forming factors. The four factors varied at three levels are wall angle, tool size, material thickness and incremental step size. The responses to the factors are the thinning rate and the maximum punch load. The Box–Behnken design can analyze four factors in three levels in a total number of 27 numerical simulation runs performed. The first objective of the set of numerically simulated tests is to define the most critical forming parameters in SPIF. The second objective is that a Box–Behnken experimental design is used to determine the affect of process parameters on the considered responses, and also it can be employed to develop mathematical models in view to define approximations of objectives functions. The forming factors and levels are listed in Table 1. In the used Box–Behnken design, the numerical process parameters are coded, in this case there are three levels codes and the coded factors are low (−1), medium (0), and high (1).

3.1 Considered DoE

Table 2 illustrates the matrix of experiments which represents the numerical data obtained based on the finite element described earlier. This experimental design was used for the optimization procedure and for the visualization of the results in the form of different graphics. It will lead to the development of an analytical formulation connecting the response to the various factors conducing to the optimization of single point incremental forming process. Consequently, this technique is suitable for exploring quadratic response surfaces and constructing second-order polynomial models.

Table 1 The levels of factors for numerical experiments

Name	Description	Inferior born (−1)	Middle (0)	Superior born (1)
α (°)	Wall angle	50	60	70
D (mm)	Punch diameter	10	17.5	25
Th_{ini} (mm)	Initial thickness	0.85	1.425	2
In (mm)	Step size	0.5	1.25	2

Table 2 Box–Behnken design of experiments

N°	α	D	Th_{ini}	In	Th final	Thinning rate	Fmax
1	0	1	0	−1	0.56	60.70 %	950
2	−1	0	1	0	1.082	45.90 %	1,600
3	−1	0	−1	0	0.46	45.88 %	475
4	1	0	−1	0	0.243	71.42 %	650
5	1	0	1	0	0.568	71.61 %	1,850
6	0	1	0	1	0.524	63.23 %	1,300
7	0	−1	0	−1	0.604	57.61 %	600
8	0	0	0	0	0.585	58.93 %	1,125
9	0	−1	0	1	0.57	60.00 %	1,000
10	0	0	−1	1	0.332	60.95 %	620
11	0	0	0	0	0.585	58.93 %	1,125
12	0	0	−1	−1	0.351	58.68 %	450
13	0	0	1	−1	0.82	59.00 %	1,250
14	1	−1	0	0	0.426	70.14 %	1,100
15	0	0	1	1	0.78	61.00 %	1,900
16	1	1	0	0	0.399	72.00 %	1,250
17	−1	−1	0	0	0.784	45.02 %	800
18	−1	1	0	0	0.77	45.96 %	940
19	1	0	0	1	0.4	71.93 %	1,350
20	0	1	−1	0	0.339	60.12 %	575
21	0	−1	−1	0	0.36	57.65 %	460
22	0	−1	1	0	0.845	57.75 %	1,300
23	0	0	0	0	0.585	58.93 %	1,125
24	1	0	0	−1	0.412	71.09 %	900
25	−1	0	0	−1	0.791	44.49 %	750
26	−1	0	0	1	0.742	47.93 %	1,200
27	0	1	1	0	0.782	60.90 %	1,850

3.2 Main effects plot of the factors

In order to compare the impacts of various factors on the value of thinning rate of the sheet and the maximum punch load, the main effects of the factors were represented in Fig. 5. It is then immediately possible to note that changes carried out between the low and high levels of different parameters affect in a more or less important way the variation of the geometrical or mechanical response according to the factors considered. The graphs of the main effects emphasize immediately the significant factors, the wall angle and the initial thickness. The variables diameter and vertical increment of the tool seem to be the factors with much less important effects on the responses.

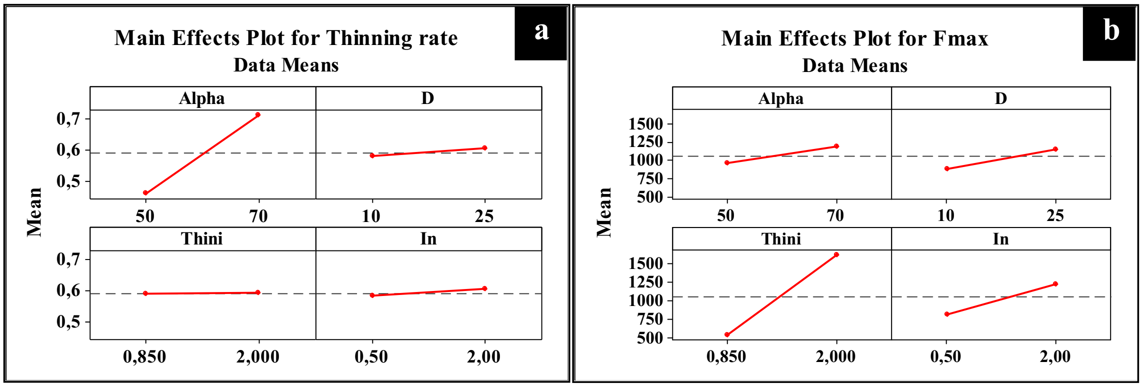

Fig. 5 Graphs of the main effects of four studied factors for: **a** thinning rate and **b** Fmax

In the presence of a significant number of factors, the construction of graphs like interaction matrix can offer an interesting alternative to the main effects of forming parameters and their interactions. Figure 6a, b shows a graphic representation of interaction plots corresponding for the two responses, respectively: the thinning rate and the maximum punch force. From the reading of the interaction plots (Fig. 6a) related to the thinning rate, the predominance of the wall angle, which appears first, can be seen. The increase in this factor contributes to grow the response values of the sheet thinning rate, that means a decrease in sheet formability. In particular, the forming angle is particularly significant for the formability when its value is larger. By eliminating the first dominating factor, we identify the influence of the other factors as well as their interactions. The interaction between tool size (or initial thickness of material) and step size is relatively nonsignificant.

The interaction effects of the process parameters corresponding to the maximum punch load are presented in graphical form given by Fig. 6b. According to this figure, the value of the response results to be strongly influenced by the initial sheet thickness parameter which affects more the punch load during the incremental forming. Indeed, this can be explained by the effects of material increasing when the thickness evolves. Therefore, the punch will be subjected to a significant quantity of material pushed to deform it, and consequently a rise in the load necessary for deforming the part will be generated. The combination of higher sheet thickness and larger values of tool diameter (or incremental step size) contributes to significant increase of the maximum force value provided by punch tool as illustrated in Fig. 6b. It should also be mentioned from the obtained interaction plots, that the interaction of the wall inclination angle with all other factors has more or less negligible effect on the output variable.

Based on the preceding results, the RSM will be used in the following section to construct the global approximation of the responses at various sampled points of design space. Therefore, MATLAB based programs were developed in this work for which all computations were carried out. Two optimization problems are formulated and two optimization procedures based on the global approach and the genetic algorithm are proposed and applied to find the optimum solutions.

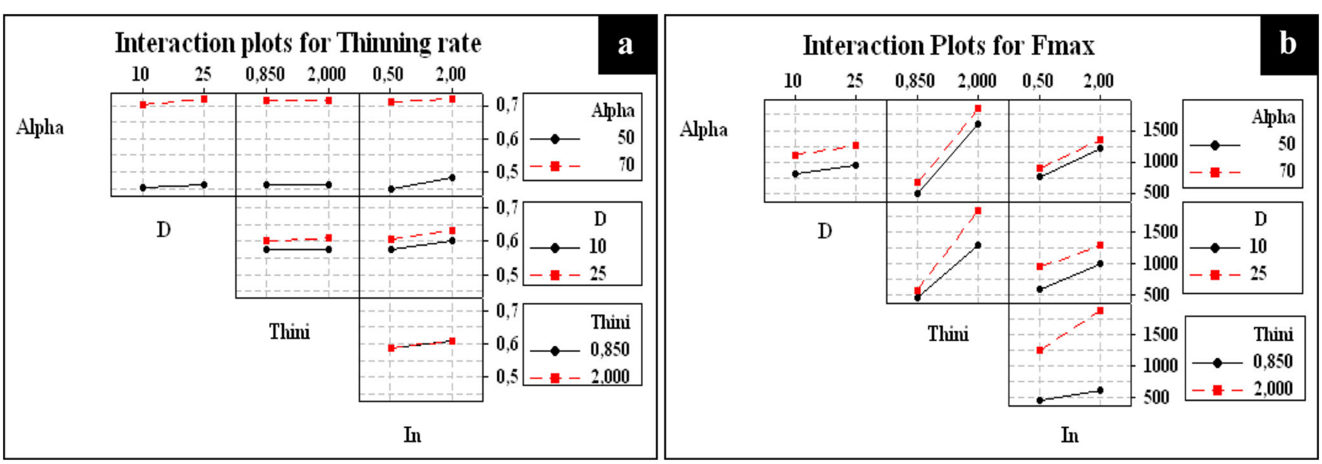

Fig. 6 The interaction effects of the input parameters for: **a** thinning rate and **b** maximum punch load

4 Procedures of optimization

In incremental forming processes of sheet metal, various criteria must be satisfied, and the search for an optimal solution can account for contradictory criteria. Consequently, several constraints and objective functions are necessary in order to obtain proper quality product.

The goal of the optimization is to get the best combination of process or geometry design variables which will lead to a desired sheet metal part without any defects, such as, maximum sheet metal thinning, fractures, insufficient stretching and thickness varying, high values of punch load, etc.

4.1 Overview of response surface approximation

For the most of the response surfaces, the functions for the approximations are polynomials because of simplicity, though the functions are not limited to the polynomials. For the cases of quadratic polynomials, the response surface function is described as follows:

$$y = \beta_0 + \sum_{j=1}^{k} \beta_j x_j + \sum_{j=1}^{k} \beta_{jj} x_j^2 + \sum_{i=1}^{k-1} \sum_{j=i+1}^{k} \beta_{ij} x_i x_j \tag{3}$$

where k is the number of design variables. In the case that total number of experiments is n, corresponding to n combinations of the design variables, the response surface can be expressed as follows by matrix expression:

$$\mathrm{Y} = \mathrm{X}\beta + \varepsilon \tag{4}$$

where

$$\mathrm{Y} = \begin{bmatrix} y_1 \\ y_2 \\ y_3 \\ \vdots \\ y_n \end{bmatrix}, \mathrm{X} = \begin{bmatrix} 1 & x_{11} & x_{12} & \cdots & x_{1k} \\ 1 & x_{21} & x_{22} & \cdots & x_{2k} \\ 1 & x_{31} & x_{32} & \cdots & x_{3k} \\ \vdots & \vdots & \vdots & \ddots & \vdots \\ 1 & x_{n1} & x_{n2} & \cdots & x_{nn} \end{bmatrix}, \beta = \begin{bmatrix} \beta_1 \\ \beta_2 \\ \beta_3 \\ \vdots \\ \beta_n \end{bmatrix}, \varepsilon = \begin{bmatrix} \varepsilon_1 \\ \varepsilon_2 \\ \varepsilon_3 \\ \vdots \\ \varepsilon_n \end{bmatrix} \tag{5}$$

In which Y is the response vector, X is the matrix of the independent variables, β is the vector of the unknown coefficients β_i and ε is the random error vector of the approximation.

The unbiased estimator ε of the coefficient vector β is obtained using the well-known least square error method as follows:

$$\mathrm{b} = \left(\mathrm{X}^{\mathrm{T}}\mathrm{X}\right)^{-1}\mathrm{X}^{\mathrm{T}}\mathrm{Y} \tag{6}$$

The variance–covariance matrix of the b is obtained as follows:

$$\mathrm{cov}\left(\mathrm{b_i}, \mathrm{b_j}\right) = \mathrm{C_{ij}} = \sigma^2\left(\mathrm{X}^{\mathrm{T}}\mathrm{X}\right)^{-1} \tag{7}$$

where the σ is the error of Y. The estimated value of σ is obtained as follows:

$$\sigma^2 = \frac{\mathrm{SS_E}}{\mathrm{n}-l-1} \tag{8}$$

where l is the number of non-consist terms in RS model, $\mathrm{SS_E}$ is a square sum of errors, and expressed as follows:

$$\mathrm{SS_E} = \mathrm{Y^T Y} - \mathrm{b^T X^T Y} \tag{9}$$

Statistical analysis techniques such as ANOVA can be used to check the fitness of RS model and to identify the main effects of design variables. The major statistical parameters used for evaluating model fitness are the Y statistic, R^2, adjusted $R^2(R^2_{\mathrm{adj}})$, and root mean square error (RMSE). Note that these parameters are not totally independent of each other and are calculated as

$$F = \frac{(\mathrm{SS_{YY}} - \mathrm{SS_E})/l}{\mathrm{SS_E}/(n-l-1)} \tag{10}$$

$$R^2 = 1 - \frac{\mathrm{SS_E}}{\mathrm{SS_{YY}}} \tag{11}$$

$$R^2_{\mathrm{adj}} = 1 - \frac{\mathrm{SS_E}/(n-l-1)}{\mathrm{S_{YY}}/n-1} \tag{12}$$

$$\mathrm{RMSE} = \sqrt{\frac{\mathrm{SS_E}}{n-l-1}} \tag{13}$$

where $\mathrm{S_{YY}}$ is the total sum of squares expressed as following, $\mathrm{SS_E}$ is presented in Eq. 9.

$$\mathrm{S_{YY}} = \mathrm{Y^T Y} - \frac{\sum_{i=1}^{n} \mathrm{y}_i}{n} \tag{14}$$

R^2 is the proportion of variability in a data set that is accounted for by a statistical model. In this case R^2 increases as we increase the number of variables in the model (R^2 will not decrease). This illustrates a drawback to one possible use of R^2, where one might try to include more variables in the model until "there is no more improvement". This leads to the alternative approach of looking at the adjusted R^2. The explanation of this statistic is almost the same as R^2 but it penalizes the statistic as extra variables are included in the model. In situations where the number of design variables is large, it is more appropriate to look at R^2_{adj}; because R^2 always increases as the number of terms in the model is increased while R^2_{adj} actually decreases if unnecessary terms are added to the model. In addition to these statistics, the accuracy of the RS model can also be measured by checking its predictability of response using the prediction error sum of squares (PRESS) and R^2 for prediction (R^2_{pred}). The PRESS statistic and R^2_{pred} are calculated as

$$\mathrm{PRESS} = \mathrm{Y}^{\mathrm{T}}\mathrm{Y} - \frac{\sum_{i=1}^{n} \mathrm{y}_{(i)}}{n} \tag{15}$$

$$R^2_{\mathrm{pred}} = 1 - \frac{\mathrm{PRESS}}{\mathrm{SS}_{\mathrm{YY}}} \tag{16}$$

where $y_{(i)}$ is the predicted value at the ith design point using the model created by $(n-l)$ design points that exclude the ith point.

4.2 Analysis of variance

The adequacy of the developed models were tested using the ANOVA technique and the results of the quadratic order response surface model fitting in the form of ANOVA are given in Tables 3 and 4. The test for significance of the regression models, the test for significance on individual model coefficients and the lack-of-fit test were performed using the same statistical Minitab 16 software package. These tables summarize the analysis of variance for each response and show the significant model terms. The same tables show the other adequacy measures R^2, adjusted R^2 and predicted R^2. The coefficient of determination R^2 indicates the goodness of fit for the model. In this case, all the values of the entire adequacy measures are nearly equal to 1, which is in reasonable agreement and indicates adequate models. Clearly, we must have $0 \le R^2 \le 1$, with larger values being more desirable. The adjusted coefficient of determination R^2 or "adjusted" R^2 is a variation of the ordinary R^2 statistic that reflects the number of factors in the model. The entire adequacy measures are closer to 1 for the two considered responses: the thinning rate and the maximum punch load, which is in reasonable agreement and indicate adequate models. Tables 3 and 4 also indicate that the predicted correlation coefficients values (predicted R^2=99.04 % and 94.16 %) for accuracy of this model are very satisfactory.

Finally, and according to the values of R^2, adjusted R^2 and predicted R^2, the response surface statistical analysis highlighted that a quadratic model well describes these two responses evolution with respect to the input data with a performance index (R^2=99.83 %, adjusted R^2=99.64 % and predicted R^2=99.04 %) and (R^2=98.99 %, adjusted R^2=97.80 % and predicted R^2=94.16 %). They correspond to the sheet thinning rate and the punch force cost functions respectively, thus confirming the results consistency.

4.3 Genetic algorithm

The genetic algorithm is a method for solving both constrained and unconstrained optimization problems that is based on natural selection, the process that drives biological evolution. The genetic algorithm repeatedly modifies a population of individual solutions. At each step, the genetic algorithm selects individuals at random from the current population to be parents and uses them produce the children for the next generation. Over successive generations, the population "evolves" toward an optimal solution. The genetic algorithm uses three main types of rules at each step to create the next generation from the current population:

- *Selection rules* select the individuals, called "parents", that contribute to the population at the next generation.
- *Crossover rules* combine two parents to form children for the next generation.
- *Mutation rules* apply random changes to individual parents to form children.

4.3.1 Genetic algorithm steps

In short, the steps involved in the GA used in this research are as follows:

Step 1 Choose a coding to represent problem parameters, a selection operator, a crossover operator, and a mutation operator. Choose population size N_{pop}, crossover probability P_c, and mutation probability P_m. Choose a maximum allowable generation GEN and initialize a random population P_0 of chromosomes.

Step 2 Evaluate fitness of the solution set for all chromosomes in the initial population. Assign a fitness value to each solution in P_0 according to the objective function.

Step 3 If a termination criterion is satisfied, terminate.

Step 4 While no termination condition, perform reproduction on the population. Select individual for mating pool members of population size set by focusing on the fitness value.

Table 3 ANOVA table for thinning rate quadratic model

Source	Degree of freedom	Sum of squares	Adjusted sum of squares	Adjusted mean square	F value	p value Prob>F
Regression	14	0.199738	0.199738	0.014267	513.12	0.000
Linear	4	0.198406	0.001814	0.000454	16.31	0.000
α	1	0.195067	0.001187	0.001187	42.69	0.000
D	1	0.001811	0.000023	0.000023	0.82	0.382
Th_{ini}	1	0.000017	0.000016	0.000016	0.56	0.467
In	1	0.001510	0.000004	0.000004	0.16	0.695
Square	4	0.001129	0.001129	0.000282	10.15	0.001
$\alpha\times\alpha$	1	0.000682	0.000301	0.000301	10.84	0.006
$D\times D$	1	0.000002	0.000024	0.000024	0.86	0.373
$Th_{ini}\times Th_{ini}$	1	0.000008	0.000018	0.000018	0.65	0.436
In×In	1	0.000436	0.000436	0.000436	15.67	0.002
Interaction	6	0.000203	0.000203	0.000034	1.22	0.361
$\alpha\times D$	1	0.000021	0.000021	0.000021	0.75	0.404
$\alpha\times Th_{ini}$	1	0.000001	0.000001	0.000001	0.02	0.879
$\alpha\times$In	1	0.000168	0.000168	0.000168	6.05	0.030
$D\times Th_{ini}$	1	0.000012	0.000012	0.000012	0.42	0.532
$D\times$In	1	0.000000	0.000000	0.000000	0.02	0.896
$Th_{ini}\times$In	1	0.000002	0.000002	0.000002	0.07	0.802
Residual error	12	0.000334	0.000334	0.000028		
Lack-of-fit	10	0.000334	0.000334	0.000033		
Pure error	2	0.000000	0.000000	0.000000		
Total	26	0.200072				

R^2 =99.83 %, adjusted R^2 = 99.64 %, predicted R^2 =99.04 %, PRESS=0.001922, S= 0.00527301

(i) Tournament Selection
(ii) Roulette Wheel Selection
(iii) Elitist selection with their rates to selecting chromosomes from population P

Step 5 Alter the population by performing the genetic operators.

(i) Crossover: Applying the crossover operation for each random pair of chromosomes with probability P_c.
(ii) Mutation: Applying the mutation operation for the genes of the chromosome with probability P_m.

Step 6 Replace the current population by the resulting new population.

Step 7 Evaluate the objective function for all strings in the new generation, called offsprings and formed by either crossover operator or mutation operator.

Step 8 If the stopping criteria is satisfied, then terminate algorithm and return the best solution of the generation

Step 9 Otherwise, go back to step 4. This process will continue until the stopping of the algorithm when the value of the fitness function for the best point in the current population is less than or equal to fitness limit.

The flowchart of GA algorithm process is shown in Fig. 7.

4.3.2 Parameters of genetic algorithm

In the optimization problem of single point incremental forming process, the chromosomes are encoded in a binary string. This type of encoding is the most common, mainly because first works about GA used this type of binary code. In binary encoding, every chromosome has one binary string of bits, 0 or 1.

The first step in the implementation of any genetic algorithm is to create an initial population composed of a group of chromosomes. The initial population evolves under determined selection rules to a new state that minimizes an objective function. Therefore, in each step, the algorithm has a population of chromosomes that holds specific qualities more than the previous population. Each population or generation of chromosomes has the same size which is well-known as the population size and is denoted by N_{pop}. In the present research, the initial population is randomly generated regarding the population size in which N_{pop} is chosen to be 300.

For creating the new generation, it is required to select some chromosomes (mating pool) from the population with the latest fitness in the progress generation for recombining or creating chromosomes allied to the new generation. In this case, tournament selection is used in which the fitness of

Table 4 ANOVA table for maximum punch load quadratic model

Source	Degree of freedom	Sum of squares	Adjusted sum of squares	Adjusted mean square	*F* value	*p* value Prob>*F*
Regression	14	4,605,298	4,605,298	328,950	83.72	0.000
Linear	4	4,414,129	9,664	2,416	0.61	0.660
α	1	148,519	166	166	0.04	0.840
D	1	214,669	6,106	6,106	1.55	0.236
$\mathrm{Th_{ini}}$	1	3,542,533	503	503	0.13	0.727
In	1	508,408	2,540	2,540	0.65	0.437
Square	4	84,207	84,207	21,052	5.36	0.010
$\alpha\times\alpha$	1	6,033	6	6	0.00	0.970
$D\times D$	1	38,958	46,667	46,667	11.88	0.005
$\mathrm{Th_{ini}}\times\mathrm{Th_{ini}}$	1	8,881	948	948	0.24	0.632
In×In	1	30,334	30,334	30,334	7.72	0.017
Interaction	6	106,963	106,963	17,827	4.54	0.013
$\alpha\times D$	1	25	25	25	0.01	0.938
$\alpha\times\mathrm{Th_{ini}}$	1	1,406	1,406	1,406	0.36	0.561
$\alpha\times$In	1	0	0	0	0.00	1.000
$D\times\mathrm{Th_{ini}}$	1	47,306	47,306	47,306	12.04	0.005
$D\times$In	1	625	625	625	0.16	0.697
$\mathrm{Th_{ini}}\times$In	1	57,600	57,600	57,600	14.66	0.002
Residual error	12	47,148	47,148	3,929		
Lack-of-fit	10	47,148	47,148	4,715		
Pure error	2	0	0	0		
Total	26	4,652,446				

R^2 =98.99 %, adjusted R^2 = 97.80 %, predicted R^2 =94.16 %, PRESS=271,572, S=62.6817

current-generation chromosomes is calculated according to objective function. In what follows, the value of tournament size used in the proposed GA of this research is 5.

When the GA operators are applied, offspring chromosome may not be a feasible solution, so these solutions are corrected to be feasible. The crossover and

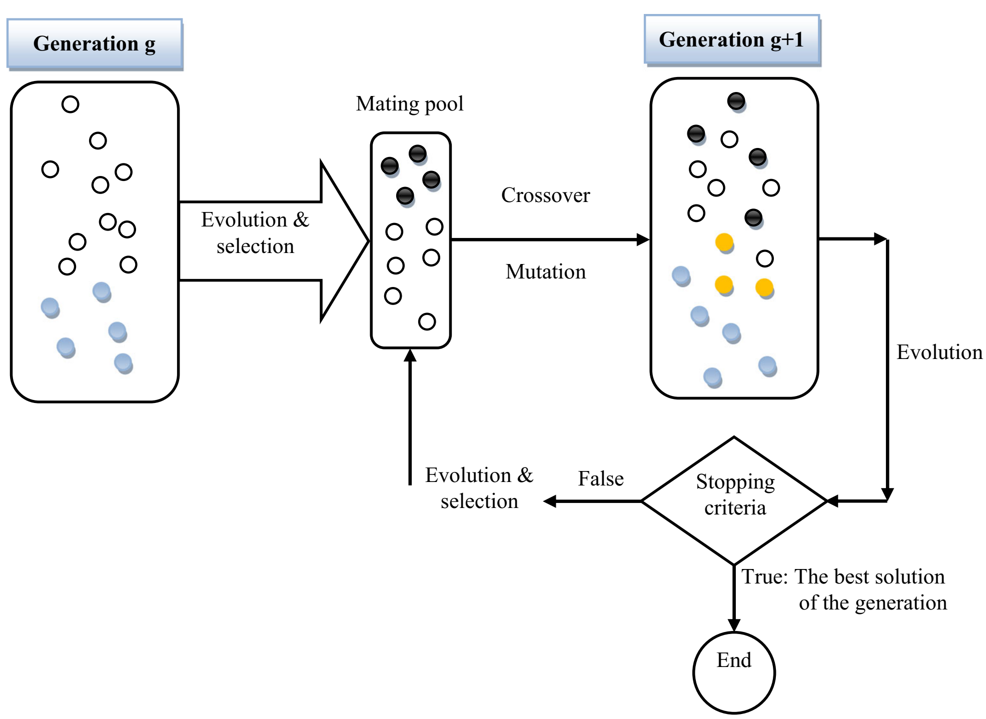

Fig. 7 The flowchart of GA algorithm process

mutation are the most important part of the genetic algorithm.

Crossover operator The crossover operator represents the main genetic operator. The last selects genes from parent chromosomes and creates a new offspring. The standard single point crossover was adopted which randomly generates one crossover points along the length of array and divides two chromosomes into two segments subsequently, from one point randomly and exchange their broken parts, resulting in two offspring's chromosomes. Crossover operates on the parents chromosomes with the probability of P_c. This parameter of crossover probability used for the GA developed here is P_c=0.9.

Mutation operator After a crossover is performed, mutation operation takes place for exploring new solutions. This operator can change the values of randomly chosen gene bits for the new offspring. Consequently, in the case of our GA the binary encoding is employed and we can switch a few randomly chosen bits from 1 to 0 or from 0 to 1. The mutation probability P_m performed in this research was chosen to be equal to its usual value of 0.01.

After producing the new chromosomes by crossover and mutation operations, we need to evaluate them. Genetic algorithm evaluates chromosomes based on fitness function value. In a minimization problem, the more appropriate the solution is the less the amount of the objective function (fitness value) will be.

The last step in a GA method is to check if the algorithm has found a solution that is good enough to meet the user's expectations. The GA uses different stopping criteria used in literature to determine the good solution. In this research the reaching a *fitness limit* of the objective function is used to stop the algorithm. At first, the algorithm examines the fitness values corresponding to the successive individuals of the present generation. The convergence error corresponding to the tolerance of the variation between two consecutive evaluations of the objective function for its convergence is chosen equal to 10^{-6}.

5 Optimization procedure based on response surface modeling

The incremental forming of metal parts is subjected to a variety of process parameters. The characteristic functions which were selected to approximate the responses of the parts during the SPIF operation are the sheet thinning rate (Thin_rate) and the maximum punch force (F_max). The effects of the interaction between the wall inclination angle (α), the punch diameter (D), the initial thickness of material (Th_{ini}) and the size of the step down (In) on the evolution of geometrical and mechanical responses were studied. Numerical and graphical optimization methods were used in this part of work by choosing the desired goals for each factor and response. For that, the RSM is used to construct global approximation of the response at various sampled points of design space. Therefore, MATLAB-based [46] programs were developed in this work for which all computations were carried out.

Polynomial regression methods are commonly used to create response surface functions from a set of sampled data. In this study, it has been found that a quadratic polynomial approximation was shown to be reliable and sufficient to fit the numerical data by using response surface methodology with less error. This quadratic order interpolation makes it possible to represent accurately two models in SPIF for the objective functions of thinning rate and maximum punch force. For a general polynomial approximation of second order, the mathematical models can be represented in the following form:

$$y = \beta_0 + \sum_{i=1}^{n} \beta_i x_i + \sum_{i=1}^{n} \beta_{ii} x_i^2 + \sum_{i<j}^{n} \beta_{ij} x_i x_j + \varepsilon \qquad (17)$$

The optimization procedure is carried out in the search range of design variables in order to determine the optimal values of these process parameters guaranteeing the minimization of sheet thinning rate (Thin_rate) and maximum punch load (F_max). The multiobjective function problem can be formulated as follows:

$$\text{Minimize} \quad \text{Thin\_rate} = F_1(\alpha, D, Th_{ini}, In) \qquad (18a)$$

$$\text{Minimize} \quad \text{F\_max} = F_2(\alpha, D, Th_{ini}, In) \qquad (18b)$$

Subject to the constraints:

$$\alpha_{min} \le \alpha \le \alpha_{max} \qquad (19a)$$

$$D_{min} \le D \le D_{max} \qquad (19b)$$

$$Th_{ini_{min}} \le Th_{ini} \le Th_{ini_{max}} \qquad (19c)$$

$$In_{min} \le In \le In_{max} \qquad (19d)$$

$\{\beta_0, \beta_i, \beta_{ii}, \beta_{ij}\}$ are the regression coefficients representing the approximate functions of the polynomials Thin_rate and F_max. They are determined by applying the method described in Section 4.1.

The theoretical development allows minimizing the square error ε_{err} between the real design point y_i and the estimated values computed by using the second-order function y. The total quadratic error is defined by:

$$\varepsilon_{\mathrm{err}} = \sqrt{\sum_{i=1}^{n_{\exp}} (y_i - y)^2} \qquad (20)$$

The minimization of the quadratic error requires the derivation of ε_{err} with respect to the constants that appears in Eq. 17. In this case, the method allows to solve a linear system in β_0, β_i, β_ii and β_ij to evaluate the objective functions Thin_rate and F_max, respectively. Tables 5 and 6 summarize the computed regression coefficients corresponding to the two polynomials of objective functions.

5.1 Response surface analysis of thinning rate objective function

RSM is the regression method exploring the relationships between several explanatory variables and one or more response variables. This technique aims at determining in a quantitative way the variations of the response function. Using the foregoing methodology, a complete set of numerical experiments was run. The results are reported in three-dimensional response surface (RS) and contour plots. The graphs given by Fig. 8a_1, b_1 are shown as the three-dimensional representation of the relative variation of the predicted thinning rate Thin_rate on the *Z*-axis and the variables: incremental step size (*X*-axis), and tool size on the *Y*-axis. From a global point of view, it worth noting in 8a_1 and 8b_1 that thinning rate of sheet metal evolves similarly. Thus, the obtained maps give a same tendency at the domain of process variables. It can be evoked, that the results show an evolution of sheet thinning in a nonlinear way according to the considered parameters and that is more sensitive to the vertical step size than to the punch diameter. These figures show that the increase in the vertical increment step size and the tool diameter represents an amplification of thinning rate of sheet metal. The minimum values of this response are located at the low ranges of process parameters wherea, high values of sheet thinning rate are reached for the most severe conditions of forming characterized by the highest values of incremental step size (In) and punch diameter (*D*). Comparing the response surface given by Fig. 8a_1 to b_1, it can be seen certainly that the thinning rate has to be affected by the wall inclination angle. Consequently, for a large value of the geometrical process parameter, the numerical result obtained for the studied response increases considerably.

The variation of thinning rate of the sheet in the space design is illustrated by contour plots shown in Fig. 8a_2, b_2, respectively for wall angle values equal to α=50° and α=70°. They make it possible to locate the regions containing the global minimum values of this response. It was found that the regions with less thinning rate are obtained in the lower left zones of last two figures corresponding to the small values of vertical step size ($\mathrm{In}_{\_\mathrm{opt}}$) and tool diameter ($D_{\_\mathrm{opt}}$). They were limited by amplitudes of $\mathrm{Thin\_rate}_{\mathrm{opt}}$=43.8094% and Thin_

Table 5 Constants of objective function of thinning rate predicted by the least squares method

Coefficients	β_0	β_1	β_2	β_3	β_4	β_{11}	β_{22}	β_{33}	β_{44}	β_{12}	β_{13}	β_{14}	β_{23}	β_{24}	β_{34}
Values	−46.6206	2.21972	−0.21691	−2.32798	2.79045	−0.00750	0.00379	0.56207	1.60815	0.00307	0.00739	−0.08667	0.03942	0.00622	−0.15652

Table 6 Constants of objective function of maximum punch load predicted by the least squares method

Coefficients	β_0	β_1	β_2	β_3	β_4	β_{11}	β_{22}	β_{33}	β_{44}	β_{12}	β_{13}	β_{14}	β_{23}	β_{24}	β_{34}
Values	−828.839	7.1449	40.88	−154.789	251.9967	−0.01042	−1.66296	40.32766	−134.074	0.03333	3.26087	9.8×10^{-15}	25.21739	−2.22222	278.261

$rate_{opt}$=69.6325%, respectively for minimum and maximum forming angle having a values of 50° and 70°.

5.2 Response surface analysis of maximum punch load objective function

A second response, which is very important, represents the maximum punch load. Indeed, the control of this response decreases the probability of the damaged parts. The global evolution of the maximum forming load F_max is illustrated by Fig. 9a_1, b_1 in form of response surfaces according to the two significant factors: incremental step size (In) and the punch diameter (*D*). Regarding the trends of the response surfaces, it is interesting to evoke the nonlinearity dependency of the maximum load according to the two retained variables and that it is more sensitive to the (*D*) than to the (In). A comparison between the response surfaces given by Fig. 9a_1, b_1, allow marking that both figures have almost the same trend, and the maximum force applied by punch is related to the mechanical resistance of the part which increases considerably with the increase in the sheet thickness. From the numerical results, it has also been deduced that the values of this mechanical response are prominent when the incremental step size (In) and the tool diameter (*D*) are high.

As mentioned in Fig. 9a_1, b_1, it can be marked that the effect of the forming load appears very significant when the difference of the maximum values of punch force corresponding to minimum and maximum initial material thickness is observed to be 620 N and 2,068 N respectively. The minimum values of the applied loads necessary for forming the part in incremental CNC sheet metal forming process are obtained for the lowest values of these process parameters. Hence, the optimal solutions are predicted for the following values defined by F_max_{opt}=302.7083N and F_max_{opt}=931.875N, when the initial thickness is maintained fixed to its lower and upper bounds equal, respectively, to Th_{ini}=0.85 mm and Th_{ini}=2 mm. The contour plots of the response surfaces are presented in Fig. 9a_2, b_2. They make it possible to locate the optimal zone in which the maximum punch load is the smallest. The regions with less punch load fitness function (F_max) are found for small values of process parameters characterized by optimal incremental step size ($In_{\_opt}$) and optimal value of punch diameter ($D_{\_opt}$).

6 Optimization results and comparison

6.1 Results of optimization by global approach

The purpose of the study is to determine the optimal relative values of process parameters which make possible to minimize sheet thinning rate Thin_rate and maximum forming

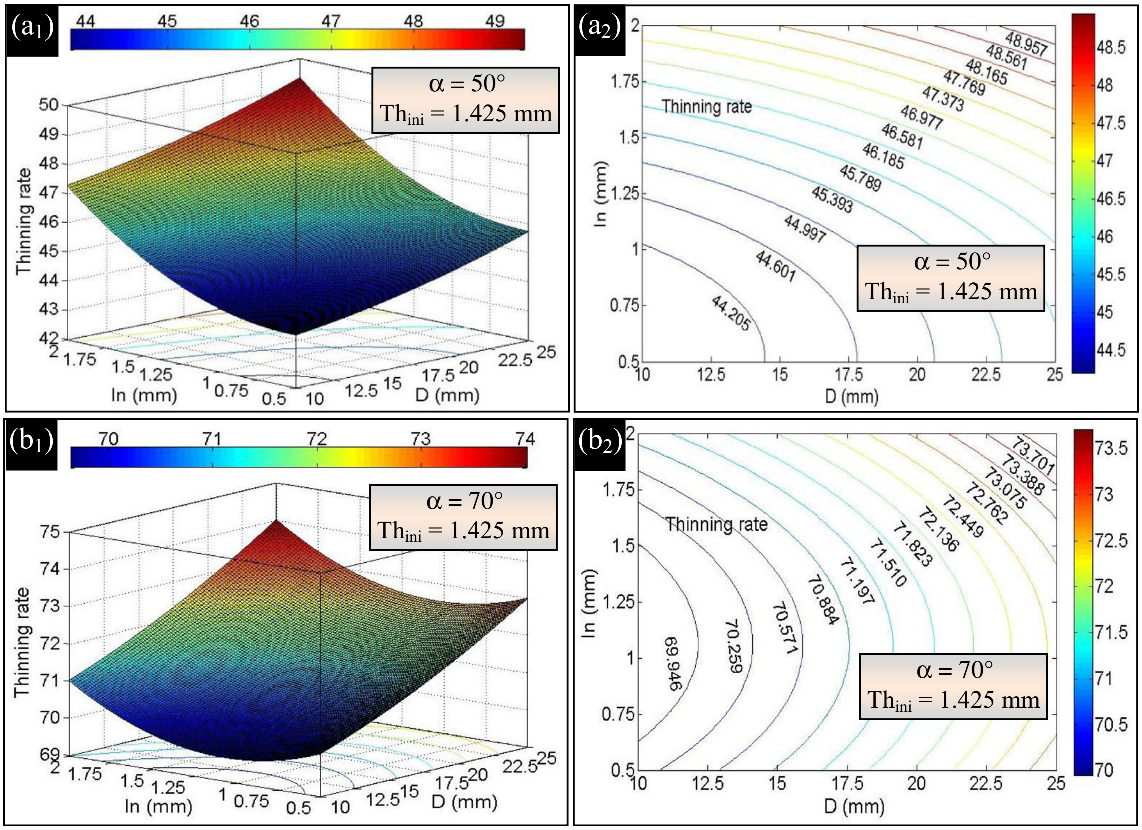

Fig. 8 Thinning rate results given in form of second-order response surfaces and contours plots of two variables. (a_1 and a_2) The wall angle α=50° (b_1 and b_2) The wall angle α=70°

load F_max. In order to do this, the four response surfaces corresponding to the two objectives functions are plotted. The optima in the global approach are found by evaluating the values of the objectives functions at points located inside the feasibility domain. The latter is sampled by a regular grid of 100×100 points which corresponds to a discretization of each process parameters. The flow chart of this optimization step is given in Fig. 10.

The minimum values of sheet thinning rate in cases of minimum and maximum values of the wall inclination angle are $\mathrm{Thin\_rate}_{\min}^{\mathrm{Global}}=43.8094\%$ and $\mathrm{Thin\_rate}_{\min}^{\mathrm{Global}}=69.6325\%$, respectively. These global minimums are reached for the following couples of process parameters: ($D_{\_opt}$= 10 mm, $\mathrm{In}_{\_opt}$=0.5300 mm) and ($D_{\_opt}$=10 mm, $\mathrm{In}_{\_opt}$=1.07 mm). This approach is applied again for the minimization of punch force cost functions. Hence, the optimal solutions corresponding to the two limit values of initial blank thickness are obtained for a minimum punch load values equal to $\mathrm{F\_max}_{\min}^{\mathrm{Global}}$= 302.7083N and $\mathrm{F\_max}_{\min}^{\mathrm{Global}}$=931.875N, respectively. The optimum process parameters provided by this global approach adopted are ($D_{\_opt}$=10 mm, $\mathrm{In}_{\_opt}$=0.5 mm) and ($D_{\_opt}$=10 mm, $\mathrm{In}_{\_opt}$=0.5 mm). The CPU time for each simulation is approximately 2 s.

6.2 Optimization results obtained using genetic algorithm

To test the algorithm's validity before its applicability to the optimization stage of single point incremental forming process, two case studies were conducted. In the first step of the analysis, the developed genetic algorithm was applied to find the minimum of Rastrigin's function, which it is often used to test the genetic algorithm, because its many local minima make it difficult for standard, gradient-based methods to find the global minimum. For two independent variables, Rastrigin's function is defined as:

$$\mathrm{Ras}(x_1, x_2) = 20 + x_1^2 + x_2^2 - 10(\cos 2\pi x_1 + \cos 2\pi x_2) \qquad (21)$$

Figure 11a. b shows the response surface and the contour plot of Rastrigin's function respectively. As shown in Fig. 11a, the plot has a lot of local minima—the "valleys" in the plot due to existing of cosine in it. However, the function has just one global minimum considered as theoretical solution, which occurs at the point [0 0] in the X1–X2 plane, as indicated by the vertical line in the plot, where the value of the function in this point is 0. The following contour plot of Rastrigin's function presented by Fig. 11b shows the alternating maxima

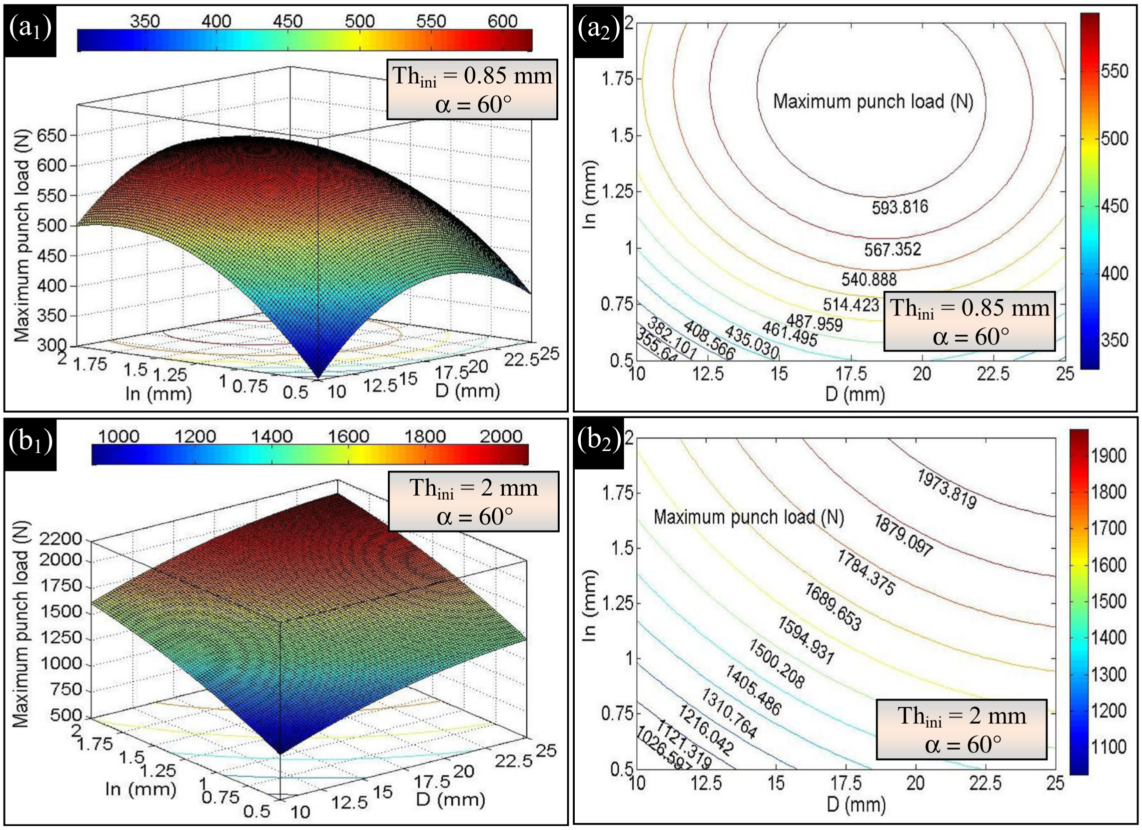

Fig. 9 Maximum punch load results given in form of second-order response surfaces and contours plots of two variables. (a_1 and a_2) The initial thickness Th_{ini}=0.85 mm (b_1 and b_2) The initial thickness Th_{ini}=2 mm

and minima. At any local minimum other than [0 0], the value of Rastrigin's function is greater than 0.

The evolution of Rastrigin's function value versus the cumulated generations number during the minimization stage is shown in Fig. 12a. Typically, the fitness value improves rapidly in the early generations, when the individuals are farther from the optimum. The best fitness value improves more slowly in later generations, whose populations are closer to the optimal point. The optimal solution of the objective function when the algorithm terminated is 0. Figure 12b displays the convergence of variables in the Rastrigin's function with the number of generation. We can note a continuous increase in the two values of variables X1 and X2 until the second iteration, and from here onwards, they begin to decrease and end up being stable. The optimal solution obtained through the optimization phase using GA was reached after six iterations corresponding to X1=−2.7914E−10 and X2=1.9974E−09. It can be concluded that the genetic algorithm provide an optimal solution very close to the theoretical solution which is considered as reference result.

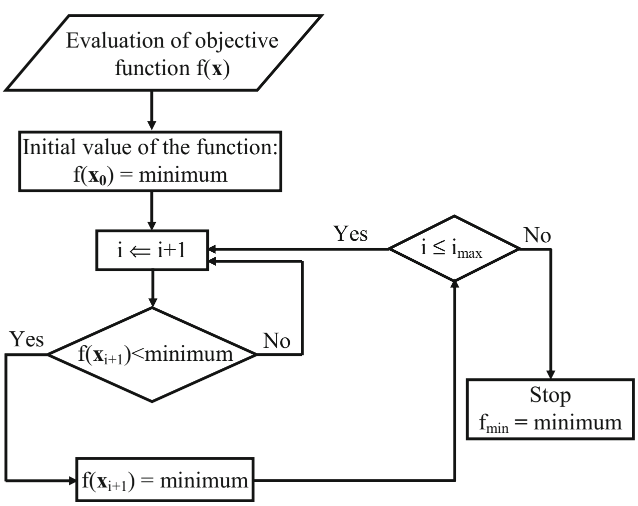

Fig. 10 Flow chart of global optimization algorithm

The second step consists in multidimensional minimization of a classic test example through a genetic algorithm. This function is Rosenbrock's function, also known as the banana function because of the way the curvature bends around the origin. The function is described by the following equation:

$$\mathrm{Ros}(x_1, x_2) = (1-x_1)^2 + 100\left(x_2-x_1^2\right)^2 \tag{22}$$

where x_1 and x_2 have a range of [−2 2;−1 3]. That is often used as a test problem for optimization algorithms. Figure 13a, b demonstrated the surface plot and the contour map of the Rosenbrock banana function metamodel approximated by RSM. As it can be seen in Fig. 13a, the Rosenbrock

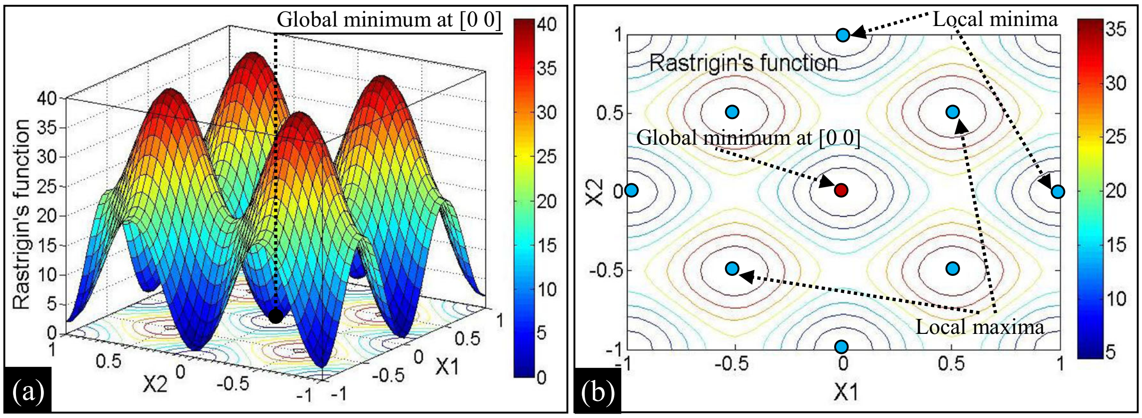

Fig. 11 A plot (**a**) and a contour plot (**b**) of Rastrigin's function

banana function has a high degree of nonlinearity and converges extremely slowly. Consequently, it is considered like a common test problem in optimization. This function has a global minimum at the point X*=[11] where it has a function value Ros(X*)=0.

The convergence history of Rosenbrock's banana function versus the number of generations during the optimization process is illustrated in Fig. 14a. According to the representative curve, it can be noticed that the objective function decreases in the first iterations and the minimal value of the response begins to be stable from the first 20 evaluations. The minimum fitness value returned by GA is approximately 1.7248E−05. Therefore, it can be observed that the value shown is comparable and very close to the global minimum represented by the theoretical solution of reference of Rastrigin's function, which is 0. Figure 14b displays the convergence history of variables of Rosenbrock's function during generations to get near an optimum point. At the begin of their evolution, each one of these two parameters presents weak fluctuations until approximately 30 generations, then from here onwards, they will be stabilized. The optimal values of the two variables are X1=0.9959 and X2=0.9917, respectively.

Comparing the minimum values of the fitness function and their optimal variables obtained in this study using a genetic algorithm with the optimum point given by the theoretical solution, an excellent agreement is obtained and the high accuracy of the joint results in this work can be clearly observed.

6.2.1 Minimization of sheet thinning rate (Thin_rate) objective functions

The first objective of the optimization procedure based on the genetic algorithm is to find the best process parameters of punch tool diameter and the vertical increment size which lead to a minimum thinning rate of sheet metal after the forming operation. The computation time required for the evaluation of every solution has been assessed to about 5 s (realized on a PC running a 2.5 GHz Core 2 Quad under Windows XP Pro and 3.96 Gb of RAM). The variation of the thinning rate objective function is plotted with the number of generation in Fig. 15a for the lower bound of the wall inclination angle of 50° and the constant initial thickness of material fixed to its average central value (Th_{ini}=1.425 mm). It can be seen that the curve decreases rapidly first and then gradually until reaching the convergence toward the minimal value of the thinning rate. The optimal solution $Thin\_rate_{min}^{GA}$=43.8094% was reached after six generations.

The convergence history of process parameters optimization to the optimal solution is illustrated in Fig. 15b. The total number of function evaluations is 42. The iterative procedure

Fig. 12 Evolution of Rastrigin's function value (**a**) and their corresponding variables (**b**) versus the number of generations during the minimization stage

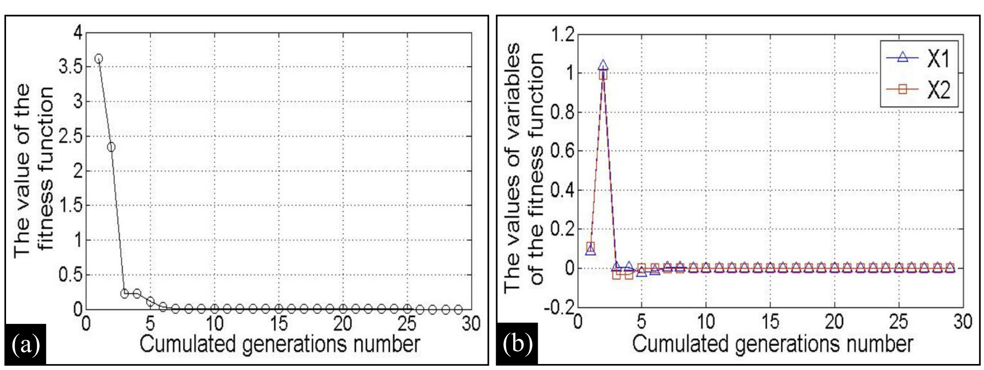

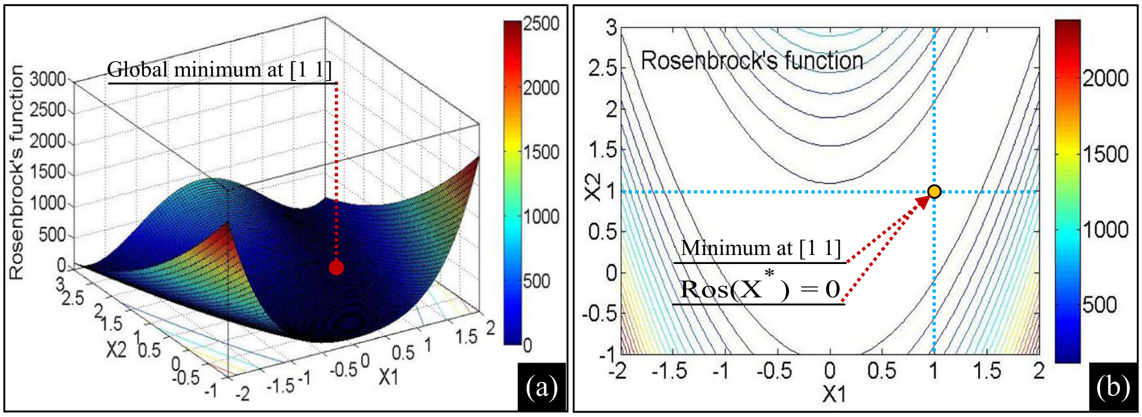

Fig. 13 A plot (**a**) and a contour plot (**b**) of Rosenbrock banana function

stops when the successive points of the objective function evaluations are superposed for a convergence with a tolerance of 10^{-6}. The process parameters optimized by the proposed optimization method defined by the values of punch diameter and vertical step size are $D_{\_opt}$=10 mm and $\text{In}_{\_opt}$= 0.5297 mm, respectively. These values can be compared with the previous results obtained through global approach to note that they are in close agreement, which will make it possible to validate the reliability and effectiveness of this genetic algorithms-based optimization process.

In the same conditions as mentioned previously, we wish to determine the optimum design variables minimizing the same fitness function of sheet thinning rate while forming the part in case of maximum wall inclination angle of 70°. The evolution of the fitness function value with the number of generation is reported in Fig. 16a. According to the representative curve, it can be noted that the minimal value of the response begins to be stable from the first five evaluations. The results of Fig. 16a show that the minimum fitness value of the objective function is $\text{Thin\_rate}_{\min}^{GA}$=69.6325%. Comparing the optimal solution of thinning rate shown by Fig. 15a for parts geometries numerically formed incrementally at 50° wall angle and the optimization result calculated by adopting a maximum slope angle α=70° described in Fig. 16a, it can be said that the sheet thinning depends strongly on the wall angle. This means that the steeper the forming angle, the greater the thinning on the sheet surface. It could be explained that when the wall angle increases, a localized nonuniform thinning however becomes more and more severe, resulting in localized thinning in the cone wall region and finally leads to unexpected failure at a certain wall angle.

The curve of the variation of incremental forming process parameters with the number of generation is plotted in Fig. 16b. According to the representative curves mentioned in the previous figure, it was found that the GA is a powerful optimization tool with respect to its robustness and its convergence speed, since these two factors present almost constant evolutions with very weak oscillations during the first iterations. In fact, this optimization technique converges to the global minimum at the point defined by the optimized values of tool diameter and incremental step size predicted by GA equal to $D_{\_opt}$=10 mm and $\text{In}_{\_opt}$=1.0686 mm, respectively.

In this part of work, some comparative studies were then carried out between all best solutions provided by the two optimization methods described previously for a better understanding of the mentioned algorithm's performance and

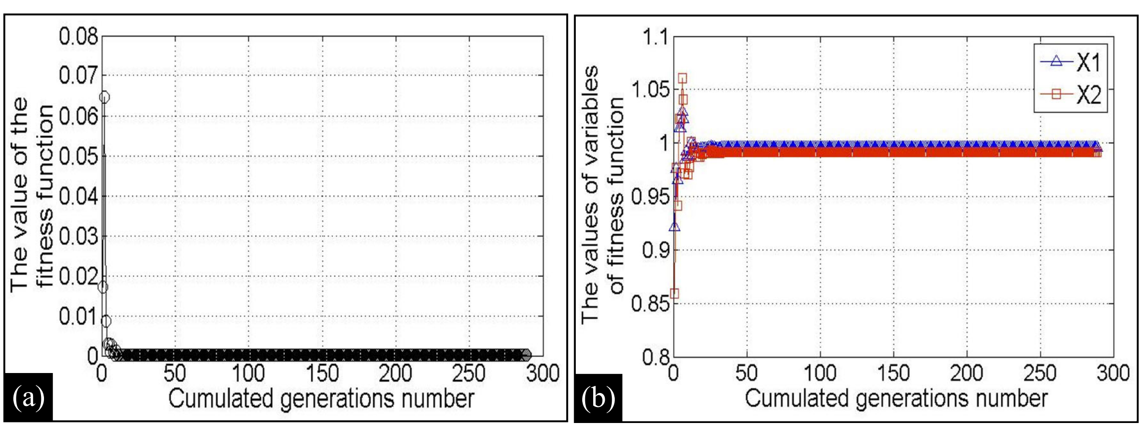

Fig. 14 Evolution of Rosenbrock's banana function value (**a**) and their corresponding variables (**b**) versus the number of generations during the minimization stage

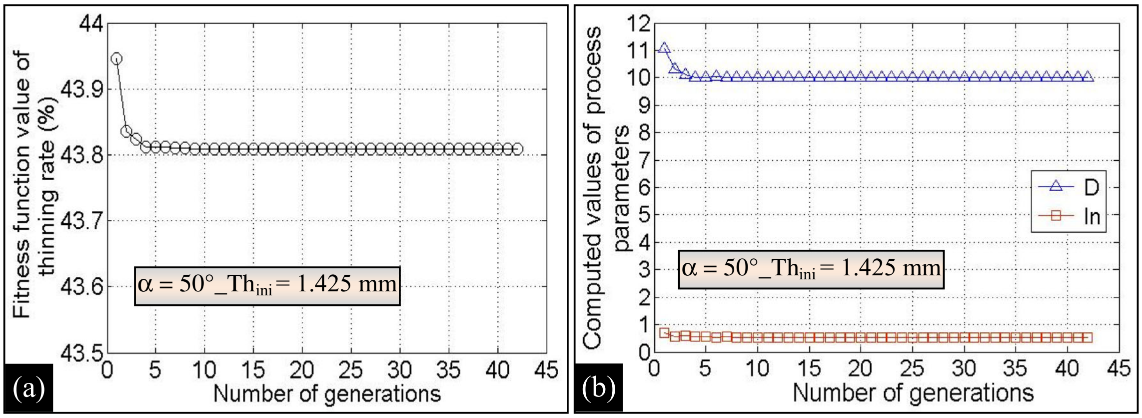

Fig. 15 Convergence history of thinning rate objective function (**a**) and process parameters (**b**) to the optimal solution with genetic algorithm in case of 50° wall inclination angle

efficiency. Table 7 recapitulates the obtained optimization results corresponding to the minimization of the thinning rate cost functions Thin_rate and the deduced optimal values of process parameters for parts formed numerically in cases of minimum and maximum values of the wall inclination angle. From Table 7, it can be seen that the numerical results of the global minimum obtained by utilizing a GA are identical to the computed values by using global approach which is considered as reference method. Consequently, these results can thus be observed as satisfactory. It can be also noticed that the optima determined by the two used optimization methods are predicted approximately at the same design points of tool diameter (*D*), and for slightly different values of the tool depth step (In).

6.2.2 Minimization of the maximum punch load (F_max) fitness functions

The second optimization problem deals with the minimization of punch load fitness function. The objective is to determine the best forming process parameters to reduce the maximum punch force predicted during the simulation of single point incremental forming operation. In the same way as previously, the genetic algorithm is employed in this stage of optimization. A graphical representation of the objective function by number of generations is shown in Fig. 17a corresponding to the lower initial sheet thickness (Th_{ini}=0.85 mm) and the forming angle maintained fixed at its medium value (α= 60°). A continuous decrease of the punch force in more or less linear according to the cumulated number of generations was observed until reaching the convergence toward its minimal value. The global optimum solution is found after the tenth iterations equal to $F\_max_{min}^{GA}$=302.7083N. The validation of the simulation is performed by comparing this optimal response value resulting form the integration of GA with the global approach based optimization technique.

In Fig. 17b, we report the convergence history of design parameters, such as the size of tool diameter as well as the vertical increment step versus the cumulated number of generations at the same time that the evaluations of the fitness function of the punch force F_max. After evolution from generation to generation, the algorithm will converge to the optimal solution defined by $D_{\_opt}$=10 mm and $In_{\_opt}$= 0.5 mm. Therefore, comparing these results obtained in this

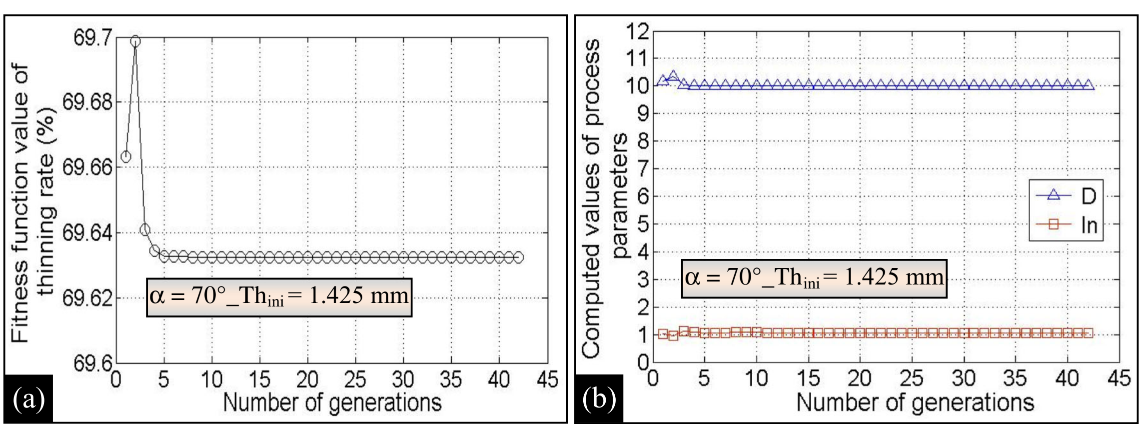

Fig. 16 Convergence history of thinning rate objective function (**a**) and process parameters (**b**) to the optimal solution with genetic algorithm in case of 70° wall inclination angle

Table 7 Summary table of the optimization results corresponding to the minimization of sheet thinning rate cost function in cases of minimum and maximum values of the wall inclination angle

Objective functions	Thinning rate for part with 50° wall angle		Thinning rate for part with 70° wall angle	
Optimization methods	Global approach	Genetic algorithm	Global approach	Genetic algorithm
Global minimum	43.8094	43.8094	69.6325	69.6325
$D_{\_opt}$	10	10	10	10
$\mathrm{In}_{\_opt}$	0.5300	0.5297	1.07	1.0686

part using a genetic algorithm to minimize the punch load objective function with the optimum parameters computed when we wish to optimize the thinning rate cost function with 50° wall angle, it can be clearly observed that they are almost identical.

The second stage consists in finding the optimum parameters which reduce the same cost function of punch load formulated for the upper limit of initial blank thickness having a value of (Th_{ini}=2 mm). For that, a similar optimization approach based on the application of the genetic algorithm was investigated. Figure 18a demonstrated the convergence path curve of the fitness function of the maximum forming force provided by tool versus cumulated evaluations number. It can be noticed that the objective function shows a rapid decrease until the third iteration then it fluctuates during the next iterations. This optimization method is well known to be efficient and to converge to a global optimum. As seen at the end of this stage, the optimal fitness value is $F\_max_{min}^{GA}$=931.875N. It was obtained after 15 iterations. As it has been observed from the previous result of optimization, an increase in the sheet thickness has a substantial impact on the magnitude of the force required for successful operation in the forming process. Consequently, it can be concluded that the numerical simulation results show that an increase in the sheet thickness also causes a considerable increase in the resultant tool force.

The established GA is adopted to optimize the process parameters with less time and faster convergence. Figure 18b represents the variation of punch diameter and vertical step size versus the generation number during the optimization phase. Initially, each one of these two parameters decreases by presenting weak fluctuations until approximately seven evaluations, then from here onwards they will be stabilized progressively to converge to an optimum solution. The converged decision variables $D_{\_opt}$ and $\mathrm{In}_{\_opt}$ are 10 and 0.5, respectively.

Table 8 presents a summary of the optimization results corresponding to the minimization of punch force cost function. It can be deduced that the two methods used lead to optimal numerical values of global response, punch diameter and step depth which are comparable and very close. It was found that all the two methods predicted the response with almost the same accuracy when the results obtained with the genetic algorithm method were also compared with the results obtained using the global approach based on the response surface method. In conclusion, the optimization strategies clearly showed their capacities to search an optimal solution with a fast convergence.

7 Conclusions and perspectives

This research focuses on the development of single point incremental sheet forming process and its optimization in order to accurately analyze the impacts of some forming

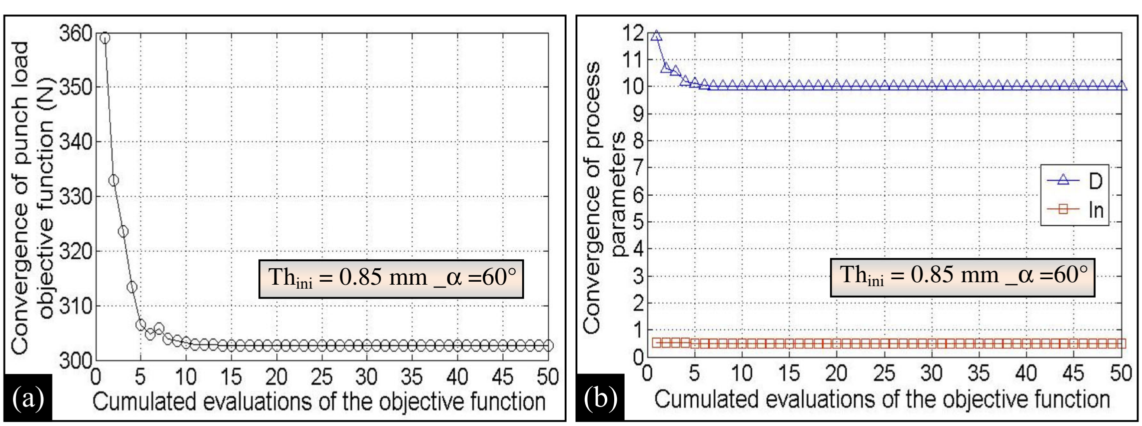

Fig. 17 Evaluation of punch load fitness function with genetic algorithm (**a**) and variation of process parameters (**b**) versus cumulated number of generations during the optimization phase for parts made from 0.85 mm initial thickness

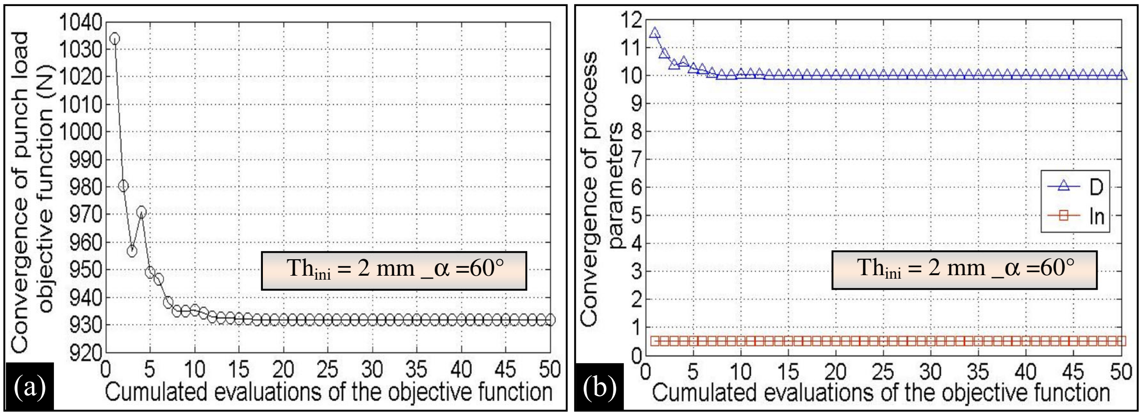

Fig. 18 Evaluation of punch load fitness function with genetic algorithm (**a**) and variation of process parameters (**b**) versus cumulated number of generations during the optimization phase for parts made from 2 mm initial thickness

factors. The proposed approach is based on finite element (FE) simulation by using the implicit algorithm of ABAQUS/Standard module. A set of numerical experiments have been conducted on SPIF, based on Box–Behnken DOE in order to determine the influence of forming angle, tool size, material thickness and step size on the sheet thinning rate and the punch loads evolution generated in this forming process. These numerical results were analyzed using statistical analysis techniques such as ANOVA to evaluate the adequacy of developed mathematical model and to check its fitness. It proves that the wall angle and the initial sheet thickness have significant effects on these two responses previously mentioned. The influences of the FE model parameters on FE results are described with a set of second-order RS. This step consists in developing of approximated objective functions in order to explore the relationship between response variables and a set of control factors. Response surface graphs and contours plots were constructed to describe the effects of the process parameters on the geometrical and mechanical responses. Also the performance of these mathematical models were served as fitness functions in minimization of maximum punch force (F_max) and sheet thinning rate (Thin_rate). In fact, two constrained optimization methodology were applied to find the optimum solutions using global approach based response surface and a developed genetic algorithm. It can be noted that the optimization method based on GA is efficient and a powerful optimization tool, since it needs not gradients and has good convergence speed. The developed approach has demonstrated its ability to efficiently optimize the incremental forming process of sheet metal. In conclusion, a comparison between the optimization results determined by this technique and the results obtained by the global approach allowed to show a good coherence between them and that the two optimal solutions are almost identical.

In terms of perspectives, some important conclusions can be stated:

- The integration of the presented methodology can be enhanced by taking into consideration the simultaneous optimization of several functions, where a problem of multiobjective robust optimization can be achieved by using a modified multiobjective genetic algorithm.
- Knowing that RSM depends strongly on the problem size and order of the approximation models; therefore, the use of RSM in conjunction with moving least square (MLS) approximation could be advantageous by considering a moving region of interest within the design space. The MLS approximation maximizes the accuracy and minimizes the number of function evaluations and consequently the number of finite element calculation. Furthermore, adaptive RSM is a technique that could be of practical use because it is able to be re-built automatically in the gradually reduced design space.

Table 8 Summary table of the optimization results corresponding to the minimization of punch force cost function in cases of minimum and maximum values of initial blank thickness

Objective functions	Punch load for part with 0.85 mm thickness		Punch load for part with 2 mm thickness	
Optimization methods	Global approach	Genetic algorithm	Global approach	Genetic algorithm
Global minimum	302.7083	302.7083	931.875	931.875
$D_{\_opt}$	10	10	10	10
$In_{\_opt}$	0.5	0.5	0.5	0.5

- Also, from an application point of view it seems important to consider real industrial parts in the future. Of course, this opens perspectives for many further investigations in this direction, mainly focused on the experimental exploration of the proposed process and on the model extension to general geometries and materials.
- A new incremental sheet forming technology with local heating will be investigated in the future to form lightweight hard-to-form sheet metals such as aluminum-magnesium alloy sheet or magnesium alloy sheet considered as attractive materials for lightweight products. Therefore, the planning of experimental studies and the development of numerical models aiming the finite element simulation of warm incremental forming at elevated temperature appear to be very interesting research orientations.

References

1. Hagan E, Jeswiet J (2003) A review of conventional and modern single point sheet metal forming methods. Proc IME B J Eng Manufact 217:213–225
2. Jeswiet J, Micari F, Hirt G, Bramley A, Duflou JR, Allwood J (2005) Asymmetric single point incremental forming of sheet metal (SheMet). Ann CIRP–Manuf Technol 54(2):623–649
3. Jeswiet J (2005) Asymmetric incremental sheet forming. Proceedings of the Eleventh International Conference on Sheet Metal (SheMet), Erlangen–Nuremberg, Germany, pp 35–58
4. Bahloul R, Arfa H, Bel Hadj Salah H (2011) Process analysis based on experimental tests and numerical modelling of single point incremental forming of sheet metal: effect of the principal process parameters. Proceedings of the XI International Conference on Computational Plasticity (COMPLAS), Barcelona, Spain
5. Ben Hmida R, Thibaud S, Gilbin A, Richard F (2013) Influence of the initial grain size in single point incremental forming process for thin sheets metal and microparts: experimental investigations. J Mater Des 45:155–165
6. Martins PAF, Bay N, Skjoedt M, Silva MB (2008) Theory of single point incremental forming. Ann CIRP–Manuf Technol 57:247–252
7. Jackson K, Allwood J (2009) The mechanics of incremental sheet forming. J Mater Process Technol 209:1158–1174
8. Hussain G, Gao L, Hayat N, Ziran X (2009) A new formability indicator in single point incremental forming. J Mater Process Technol 209:4237–4242
9. Bambach M, Ames J, Azaouzi M, Campagne L, Hirt G, Batoz JL (2005) New forming strategies for single point incremental sheet forming: experimental evaluation and numerical simulation. Proceedings of the eighth International Conference on Material Forming (ESAFORM), pp 671–674
10. Arfa H, Bahloul R, BelHadjSalah H (2012) Finite element modelling and experimental investigation of single point incremental forming process of aluminum sheets: influence of process parameters on punch force monitoring and on mechanical and geometrical quality of parts. Int J Mater Form. doi:10.1007/s12289-012-1101-z
11. Duflou JR, Tunçkol Y, Szekeres A, Vanherck P (2007) Experimental study on force measurements for single point incremental forming. J Mater Process Technol 189:65–72
12. Ambrogio G, Filice L, Micari F (2006) A force measuring based strategy for failure prevention in incremental forming. J Mater Process Technol 177:413–416
13. Ham M, Jeswiet J (2007) Single point incremental forming limits using a Box-Behnken design of experiment. Key Eng Mater 344: 629–636
14. Ham M, Jeswiet J (2007) Forming limit curves in single point incremental forming. Ann CIRP 56:277–280
15. Arfa H, Bahloul R, BelHadjSalah H (2009) Simulation numérique du formage incrémental. 19ème Congrès Français de Mécanique (CFM'2009), Marseille
16. Dejardin S, Thibaud S, Gelin JC, Michel G (2010) Experimental investigations and numerical analysis for improving knowledge of incremental sheet forming process for sheet metal parts. J Mater Process Technol 210:363–369
17. Thibaud S, Ben Hmida R, Richard F, Malécot P (2012) A fully parametric toolbox for the simulation of single point incremental sheet forming process: numerical feasibility and experimental validation. Simul Model Pract Theory 29:32–43
18. Bouffioux C, Lequesne C, Vanhove H, Duflou JR, Pouteau P, Duchêne L, Habraken AM (2011) Experimental and numerical study of an AlMgSc sheet formed by an incremental process. J Mater Process Technol 211:1684–1693
19. Bouffioux C, Henrard C, Eyckens P, Aerens R, Van Bael A, Sol H, Duflou JR, Habraken AM (2008) Comparison of the tests chosen for material parameter identification to predict single point incremental forming forces. Proceedings of IDDRG Conference, Olofström, Sweden, pp 133–144
20. Bouffioux C, Pouteau P, Duchêne L, Vanhove H, Duflou JR, Habraken AM (2010) Material data identification to model the single point incremental forming process. Int J Mater Form 3(Suppl 1):979–982. doi:10.1007/s12289-010-0933-7
21. Lequesne C, Henrard C, Bouffioux C, Duflou JR, Habraken AM (2008) Adaptive remeshing for incremental forming simulation. Proceedings of Numisheet Conference, Interlaken, Switzerland, pp 399–403
22. Henrard C, Bouffioux C, Duchene L, Duflou JR (2007) Validation of a new finite element for incremental forming simulation using a dynamic explicit approach. Key Eng Mater 344:495–502
23. Henrard C, Bouffioux C, Eyckens P, Sol H, Duflou JR, Van Houtte P, Van Bael A, Duchene L, Habraken AM (2011) Forming forces in single incremental forming: prediction by finite element simulations, validation and sensitivity. Comput Mech 47:573–590
24. Malhotra R, Huang Y, Xue L, Cao J, Belytschko T (2010) An investigation on the accuracy of numerical simulations for single point incremental forming with continuum elements. Proceedings of the tenth International Conference on Numerical Methods in Industrial Forming Processes (NUMIFORM), Pohang, Korea, 1252: 221–227
25. Bambach M, Cannamela M, Azaouzi M, Hirt G, Batoz JL (2006) Computer-aided tool path optimization for single point incremental sheet forming. Adv Meth Mater Form:234–250
26. Attanasio A, Ceretti E, Giardini C, Mazzoni L (2008) Asymmetric two points incremental forming: improving surface quality and geometric accuracy by tool path optimization. Mater Process Technol 197:59–67
27. Matthieu R, Hascoet JY, Hamann JC, Plenel Y (2009) Tool path programming optimization for incremental sheet forming applications. J Comput Aided Des 41:877–885
28. Ham M, Jeswiet J (2006) Single point incremental forming and the forming criteria for AA3003. Ann CIRP–Manuf Technol 55(1):241–244
29. Bahloul R (2011) Optimisation of process parameters in flanging operation in order to minimise stresses and Lemaitre's damage. J Mater Des 32:108–120

30. Wang H, Li GY, Zhong ZH (2008) Optimization of sheet metal forming processes by adaptive response surface based on intelligent sampling method. J Mater Process Technol 197:77–88
31. Azaouzi M, Lebaal N (2012) Tool path optimization for single point incremental sheet forming using response surface method. Simul Model Pract Theory 24:49–58
32. Attanasio A, Ceretti E, Giardini C (2006) Optimization of tool path in two points incremental forming. J Mater Process Technol 177:409–412
33. Sun G, Li G, Gong Z, Cui X, Yang X, Li Q (2010) Multiobjective robust optimization method for drawbead design in sheet metal forming. J Mater Des 31:1917–1929
34. Filice L, Ambrogio G, Micari F (2006) On-line control of single point incremental forming operations through punch force monitoring. Ann CIRP–Manuf Technol 55(1):245–248
35. Ahari H, Khajepour A, Bedi S, Melek WW (2011) A genetic algorithm for optimization of laminated dies manufacturing. J Comput Aided Des 43:730–737
36. Bahloul R, Ben Ayed L, Potiron A, Batoz JL (2010) Comparison between three optimization methods for the minimization of maximum bending load and springback in wiping die bending obtained by an experimental approach. Int J Adv Manuf Technol 48:1185–1203
37. Liu W, Liu Q, Ruana F, Liang Z, Qiu H (2007) Springback prediction for sheet metal forming based on GA-ANN technology. J Mater Process Technol 187(188):227–231
38. Wei L, Yuying Y (2008) Multi-objective optimization of sheet metal forming process using Pareto-based genetic algorithm. J Mater Process Technol 208:499–506
39. Khoei AR, Keshavarz S, Biabanaki SOR (2010) Optimal design of powder compaction processes via genetic algorithm technique. Finite Elem Anal Des 46:843–861
40. Ledoux Y, Sébastian P, Samper S (2010) Optimization method for stamping tools under reliability constraints using genetic algorithms and finite element simulations. J Mater Process Technol 210:474–486
41. Aguir H, BelHadjSalah H, Hambli R (2011) Parameter identification of an elasto-plastic behaviour using artificial neural networks-genetic algorithm method. J Mater Des 32:48–53
42. Yin F, Mao H, Hua L (2011) A hybrid of back propagation neural network and genetic algorithm for optimization of injection molding process parameters. J Mater Des 32:3457–3464
43. Fu Z, Mo J, Chen L, Chen W (2010) Using genetic algorithm-back propagation neural network prediction and finite-element model simulation to optimize the process of multiple-step incremental air-bending forming of sheet metal. J Mater Des 31:267–277
44. Van Bael A, Eyckens P, He S, Bouffioux C, Henrard C, Habraken AM, Duflou JR, Van Houtte P (2007) Forming limit predictions for single-point incremental sheet metal forming. Proceedings of the tenth International Conference on Material Forming (ESAFORM), Zaragoza, Spain
45. Bahloul R, Arfa H, BelHadjSalah H (2013) Application of response surface analysis and genetic algorithm for the optimization of single point incremental forming process. Key Eng Mater 554(557):1265–1272. doi:10.4028/www.scientific.net/KEM.554-557.1265
46. MATLAB User's guide, version 7.5.0.342 (R2007 b), (The MathWorks, Inc.)